

Novel Substituent Effect on ^{77}Se NMR Chemical Shifts Caused by 4c-6e versus 2c-4e and 3c-4e in Naphthalene Peri Positions: Spectroscopic and Theoretical Study

Satoko Hayashi and Warô Nakanishi*

Department of Material Science and Chemistry, Faculty of Systems Engineering, Wakayama University, 930 Sakaedani, Wakayama 640-8510, Japan

Received March 4, 1999

$\delta(^8\text{Se})$ values for 1-[8-(*p*- $\text{YC}_6\text{H}_4\text{Se}$) C_{10}H_6]SeSe[C $_{10}\text{H}_6$ (SeC $_6\text{H}_4\text{Y}$ -*p*)-8']-1' (**1**; Y = H, OMe, Me, Cl, Br, COOEt, and NO $_2$) showed a good correlation with those of 1-(MeSe)-8-(*p*- $\text{YC}_6\text{H}_4\text{Se}$) C_{10}H_6 (**2**). While the $\delta(^1\text{Se})$ values correlated well with $\delta(^8\text{Se})$ in **2** with a positive proportionality constant of 0.252 (regular correlation), a similar correlation for **1** gave a negative proportionality constant of -0.282 (inverse correlation). To clarify the mechanism associated with the inverse correlation in **1**, together with the regular correlation in **2**, ab initio MO calculations, containing the GIAO magnetic shielding tensor for the Se nucleus ($\sigma(\text{Se})$), were performed on *p*- $\text{YC}_6\text{H}_4\text{ASeH}$ - $^{\text{B}}\text{SeH}$ - $^{\text{B}}\text{SeH}$ - $^{\text{A}}\text{SeC}_6\text{H}_4\text{Y}$ -*p* (**3**: model of Se $_4$ 4c-6e for **1**) and on *p*- $\text{YC}_6\text{H}_4\text{ASeH}$ - $^{\text{B}}\text{SeH}_2$ (**4** and **5**: models of Se $_2$ π type 2c-4e and $^{\text{A}}\text{Se}$ - $^{\text{B}}\text{Se}$ -H 3c-4e for **2**, respectively) with the 6-311+G(2d,p) basis sets at B3LYP and/or HF levels. The characteristic nature of the substituent effects on atomic charges and $\delta(\text{Se})$ values in **3** is demonstrated to be $\text{Y}^{\delta-}\leftarrow\text{C}_6\text{H}_4\text{-Se}^{\delta+}$ - $^{\text{B}}\text{Se}^{\delta+}$ - $^{\text{B}}\text{Se}^{\delta+}$ - $^{\text{A}}\text{Se}^{\delta+}\leftarrow\text{C}_6\text{H}_4\text{-Y}^{\delta-}$ and $\text{Y}^{\delta-}\leftarrow\text{C}_6\text{H}_4\text{-Se}^{\text{down}}$ - $^{\text{B}}\text{Se}^{\text{up}}$ - $^{\text{B}}\text{Se}^{\text{up}}$ - $^{\text{A}}\text{Se}^{\text{down}}\leftarrow\text{C}_6\text{H}_4\text{-Y}^{\delta-}$, respectively, (Y = electron-withdrawing) and in **5** is $\text{Y}^{\delta-}\leftarrow\text{C}_6\text{H}_4\text{-Se}^{\delta+}$ - $^{\text{B}}\text{Se}^{\delta-}$ -H $^{\delta+}$ and $\text{Y}^{\delta-}\leftarrow\text{C}_6\text{H}_4\text{-Se}^{\text{down}}$ - $^{\text{B}}\text{Se}^{\text{down}}$ -H $^{\text{down}}$, respectively. In the case of **4**, a substantial contribution through the naphthylidene group is suggested. These results indicate that the nature of the interaction between the linear four Se atoms in **1** is of the 4c-6e type and that between the two Se atoms in **2** is π type 2c-4e and/or 3c-4e according to the conformations around the Se atoms. The observed NMR parameters are well explained by model calculations on **3**–**5**. Plots of $^4J(^1\text{Se}, ^8\text{Se})$ versus $\delta(^8\text{Se})$ of **1** and **2** gave good correlations with negative proportionality constants, which indicates that the J values become larger as the electron density on the ^8Se atoms increases.

Introduction

In our previous paper,¹ we reported the linear alignment of the four selenium atoms in bis[8-(phenylselanyl)naphthyl] diselenide (**1a**), revealed by the X-ray crystallographic analysis. This alignment is the results of an energy lowering effect due to the construction of the four center-six electron bond (4c-6e) with four selenium 4p atomic orbitals as indicated by MO calculations.¹ The character of the charge transfer in the formation of the 4c-6e is that from the p-type lone pairs of the outside two selenium atoms to the central $\sigma^*(\text{Se}-\text{Se})$ orbital. The Se–Se distance in the diselenide moiety of a model compound of **1a**, H $_2\text{Se}$ - $^{\text{H}}\text{Se}$ - $^{\text{H}}\text{Se}$ -H, is calculated to be longer than that calculated for free H $_2\text{Se}_2$.

On the other hand, X-ray crystallographic analysis of 1-(methylselanyl)-8-(phenylselanyl)naphthalene (**2a**) showed that the two Se–C bonds of the methylselanyl and phenylselanyl groups declined about 50° and 40°, respectively, from the naphthyl plane.¹ The structure **2a** in the vicinity of the Se–C bonds is reproduced by MO calculations performed on a model compound of **2a**, H $_2\text{Se}$ - $^{\text{H}}\text{SeH}_2$. The interaction of two p-type lone pairs of the Se atoms in **2a** forms two new π -type molecular orbitals, which assume an orientation that avoids the

exchange repulsion. The bent structure of **2a** must lower the energy of the filled π - and π^* -orbitals of the adduct as much as possible. The nonbonded interactions in **2a** can be represented by the π -type two-center four-electron interaction (2c-4e).¹ However, we found another type of structure,² very recently, in which the n(Se)- $\sigma^*(\text{Se}-\text{C})$ 3c-4e interaction is observed in 1-(methylselanyl)-8-(*p*-anisylselanyl)naphthalene (**2b**) and 1-(methylselanyl)-8-(*p*-chlorophenylselanyl)naphthalene (**2d**). Structures **1a**, **2a**, and **2d** are shown in Chart 1 and the corresponding orbital interactions are outlined in Chart 2, for convenience of discussion.

Lone pair–lone pair interactions have been demonstrated to play an important role in the nonbonded spin–spin couplings between selenium–selenium,^{3,4} selenium–fluorine,⁵ fluorine–fluorine,⁶ and fluorine–nitrogen⁷ atoms. The values of $^4J(\text{Se}, \text{Se})$ of **1a**,¹ **2a**,¹ 1-(acetoxymethylselanyl)-8-(methylselanyl)naphthalene,^{4b} and 1-(methylselanyl)-8-(methylselanyl)naphthalene^{4b} are reported to be 341.4, 322.4, 310, and 203 Hz, respectively. The values of $^4J(\text{F}, \text{Se})$ and $^4J(\text{F}, \text{F})$ in 8-fluoro-1-(*p*-anisylselanyl)-

(2) Nakanishi, W.; Hayashi, S. Unpublished results.

(3) Nakanishi, W.; Hayashi, S.; Yamaguchi, H. *Chem. Lett.* **1996**, 947.

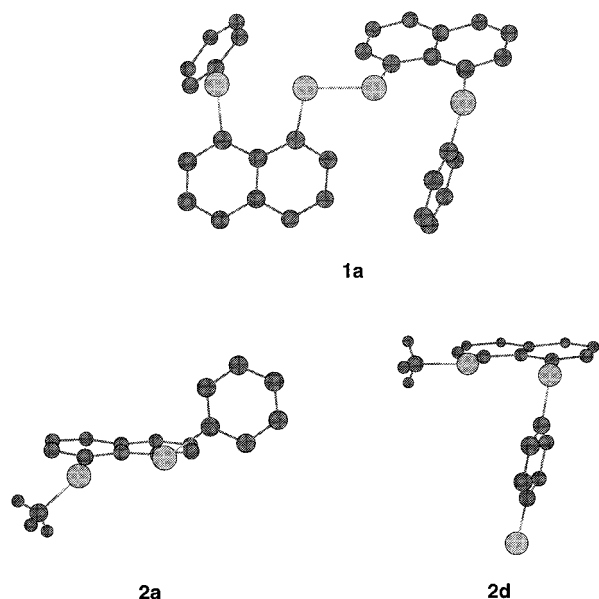
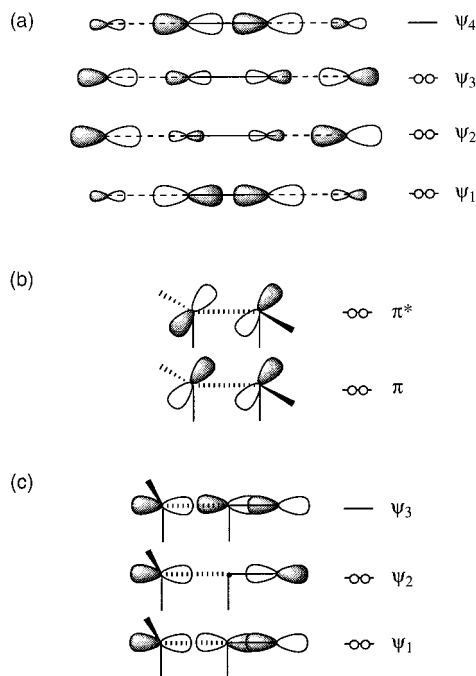
(4) (a) Johannsen, I.; Eggert, H. *J. Am. Chem. Soc.* **1984**, *106*, 1240. Johannsen, I.; Eggert, H.; Gronowitz, S.; Hörnfeldt, A.-B. *Chem. Scr.* **1987**, *27*, 359. Fujihara, H.; Mima, H.; Erata, T.; Furukawa, N. *J. Am. Chem. Soc.* **1992**, *114*, 3117. (b) Fujihara, H.; Saito, R.; Yabe, M.; Furukawa, N. *Chem. Lett.* **1992**, 1437.

(5) Nakanishi, W.; Hayashi, S.; Sakaue, A.; Ono, G.; Kawada, Y. *J. Am. Chem. Soc.* **1998**, *120*, 3635.

* To whom correspondence should be addressed. Tel: +81-734-57-8252. Fax: +81-734-57-8253 or +81-734-57-8272. E-mail: nakanishi@sys.wakayama-u.ac.jp.

(1) Nakanishi, W.; Hayashi, S.; Toyota, S. *J. Org. Chem.* **1998**, *63*, 8790. See also: Nakanishi, W.; Hayashi, S.; Toyota, S. *J. Chem. Soc., Chem. Commun.* **1996**, 371.

Chart 1. Structures 1a, 2a, and 2d

Chart 2. Interactions between Lone Pairs of Se Atoms: (a) Linear 4c-6e Constructed by Four Se Atoms, (b) π Type Se---Se 2c-4e, and (c) Linear Se---Se-C 3c-4e

naphthalene,⁵ 8-fluoro-1-(methylselanyl)naphthalene,⁵ and 1,8-difluoronaphthalene^{6b} are observed to be 285.0, 276.7, and 58.8 Hz, respectively. Orientation of the lone pairs at the Se atoms and/or electron densities of the orbitals must play an important role in determining the J values.

(6) (a) Mallory, F. B. *J. Am. Chem. Soc.* **1973**, *95*, 7747. (b) Mallory, F. B.; Mallory, C. W.; Fedarko, M.-C. *J. Am. Chem. Soc.* **1974**, *96*, 3536. (c) Mallory, F. B.; Mallory, C. W.; Ricker, W. M. *J. Am. Chem. Soc.* **1975**, *97*, 4770. Mallory, F. B.; Mallory, C. W.; Ricker, W. M. *J. Org. Chem.* **1985**, *50*, 457. Mallory, F. B.; Mallory, C. W.; Baker, M. B. *J. Am. Chem. Soc.* **1990**, *112*, 2577. (d) Ernst, L.; Ibrom, K. *Angew. Chem., Int. Ed. Engl.* **1995**, *34*, 1881. Ernst, L.; Ibrom, K.; Marat, K.; Mitchell, R. H.; Bodwell, G. J.; Bushnell, G. W. *Chem. Ber.* **1994**, *127*, 1119.

(7) Mallory, F. B.; Luzik, E. D., Jr.; Mallory, C. W.; Carroll, P. J. *J. Org. Chem.* **1992**, *57*, 366. Mallory, F. B.; Mallory, C. W. *J. Am. Chem. Soc.* **1985**, *107*, 4816.

The structure of **2a** is very close to that of 1,8-bis-(methylthio)naphthalene⁸ and of 1,8-bis(phenyltelluro)naphthalene,⁹ especially in the vicinity of the heteroatoms. Influence of the lone pair-lone pair interactions on the NMR chemical shifts is also of interest.^{5,10}

As an extension of our study, we looked for novel properties that arose from the 4c-6e-type interaction constructed by the linearly aligned four Se atoms in **1a**. The properties of the π type 2c-4e in **2a** and the linear 3c-4e in **2d** were also of interest. It was desirable that the ^{77}Se NMR chemical shifts were predicted precisely from theoretical considerations. Magnetic shielding tensors have recently been calculated based on the gauge including atomic orbital (GIAO) theory for some nuclei of the first- and second-row elements.^{11,12} The contribution of relativistic terms has been pointed out for the heavier atoms in such calculations;¹³ however, the contribution to the Se nucleus is expected to be small. The method is satisfactorily applied on organoselenium compounds¹⁴ containing para-substituted phenyl selenides.¹⁵

Ab initio MO calculations, containing the GIAO magnetic shielding tensor of the selenium nucleus ($\sigma(\text{Se})$), were performed on the model adducts of the diselenides and the bis-selenides to elucidate the nature of the nonbonded interactions characteristic of the 4c-6e, 2c-4e, and 3c-4e types. Here, we would like to present the results of investigations exhibiting the characteristic substituent effect on the Se atoms in 4c-6e in **1**, in contrast to that of 2c-4e and/or 3c-4e in **2**. The interpretation of the nonbonded interactions in **1a**, **2a**, and their derivatives based on the MO calculations is further examined.

Results and Discussion

Substituent Effect on ^{77}Se NMR Chemical Shifts and Coupling Constants. Di(para-substituted phe-

(8) (a) Glass, R. S.; Andruski, S. W.; Broeker, J. L. *Rev. Heteroatom Chem.* **1988**, *1*, 31. Glass, R. S.; Andruski, S. W.; Broeker, J. L.; Firouzabadi, H.; Steffen, L. K.; Wilson, G. S. *J. Am. Chem. Soc.* **1989**, *111*, 4036. (b) Glass, R. S.; Adamowicz, L.; Broeker, J. L. *J. Am. Chem. Soc.* **1991**, *113*, 1065.

(9) Fujihara, H.; Ishitani, H.; Takaguchi, Y.; Furukawa, N. *Chem. Lett.* **1995**, 571.

(10) (a) Goldstein, B. M.; Kennedy, S. D.; Hennen, W. J. *J. Am. Chem. Soc.* **1990**, *112*, 8265. (b) Barton, D. H. R.; Hall, M. B.; Lin, Z.; Parekh, S. I.; Reibenspies, J. *J. Am. Chem. Soc.* **1993**, *115*, 5056.

(11) Cheeseman, J. R.; Trucks, G. W.; Keith, T. A.; Frisch, M. J. *J. Chem. Phys.* **1996**, *104*, 5497.

(12) (a) Forsyth, D. A.; Sebag, A. B. *J. Am. Chem. Soc.* **1997**, *119*, 9483. (b) Olah, G. A.; Shamma, T.; Burrichter, A.; Rasul, G.; Prakash, G. K. S. *J. Am. Chem. Soc.* **1997**, *119*, 12923; Olah, G. A.; Shamma, T.; Burrichter, A.; Rasul, G.; Hachoumy, M.; Prakash, G. K. S. *J. Am. Chem. Soc.* **1997**, *119*, 12929.

(13) Tanaka, S.; Sugimoto, M.; Takashima, H.; Hada, M.; Nakatsuji, H. *Bull. Chem. Soc., Jpn.* **1966**, *69*, 953. Ballard, C. C.; Hada, M.; Kaneko, H.; Nakatsuji, H. *Chem. Phys. Lett.* **1996**, *254*, 170. Nakatsuji, H.; Hada, M.; Kaneko, H.; Nakajima, T. *Chem. Phys. Lett.* **1996**, *255*, 429. Hada, M.; Kaneko, H.; Nakatsuji, H. *Chem. Phys. Lett.* **1996**, *261*, 7. Nakatsuji, H.; Hu, Z.-M.; Nakajima, T. *Chem. Phys. Lett.* **1997**, *275*, 429. See also references cited therein.

(14) (a) Nakatsuji, H.; Higashioji, T.; Sugimoto, M. *Bull. Chem. Soc. Jpn.* **1993**, *66*, 3235. (b) Magyarfalvi, G.; Pulay, P. *Chem. Phys. Lett.* **1994**, *225*, 280. (c) Bühl, M.; Gauss, J.; Stanton, J. F. *Chem. Phys. Lett.* **1995**, *241*, 248. (d) Bühl, M.; Thiel, W.; Fleischer, U.; Kutzelnigg, W. *J. Phys. Chem.* **1995**, *99*, 4000. (e) Malkin, V. G.; Malkina, O. L.; Casida, M. E.; Salahub, D. R. *J. Am. Chem. Soc.* **1994**, *116*, 5898. (f) Schreckenbach, G.; Ruiz-Morales, Y.; Ziegler, T. *J. Chem. Phys.* **1996**, *104*, 8605. (g) Ellis, P. D.; Odom, J. D.; Lipton, A. S.; Chen, Q.; Gulick, J. M. In *Nuclear Magnetic Shieldings and Molecular Structure*; Tossel, J. A., Ed.; NATO ASI Series; Kluwer Academic Publishers: Dordrecht, 1993; p 539. See also references cited therein.

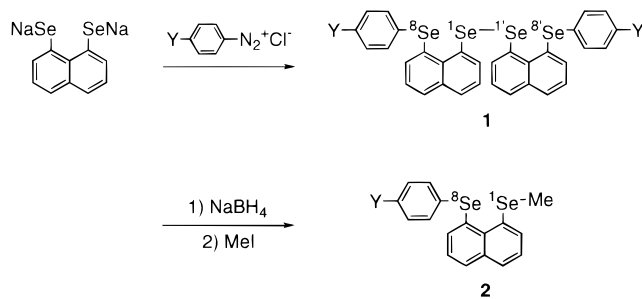
(15) (a) Nakanishi, W.; Hayashi, S. *Chem. Lett.* **1998**, 523. (b) Nakanishi, W.; Hayashi, S. *J. Phys. Chem.*, in press.

Table 1. ^{77}Se NMR Chemical Shifts and Coupling Constants of **1** and **2**, Together with the Selected ^{13}C Chemical Shifts and Coupling Constants^a

Y	1				2 ^b				
	$\delta(^8\text{Se})$	$\delta(^1\text{Se})$	$^4J(^8\text{Se}, ^1\text{Se})$	$^5J(^8\text{Se}, ^1\text{Se})$	$\delta(^8\text{Se})$	$\delta(^1\text{Se})$	$^4J(^8\text{Se}, ^1\text{Se})$	$\delta(\text{C}_{\text{Me}})$	$^1J(^1\text{Se}, \text{C}_{\text{Me}})$
OMe	416.2	541.4	371.6	12.4	424.5	233.1	341.6	13.9	71.2
Me	422.0	537.4	354.4	11.9	427.7	234.5	330.9	13.7	72.8
H	429.0	534.2	341.4	13.6	434.3	235.4	322.4	13.4	72.8
Cl	429.1	534.7	330.1	14.0	431.6	234.7	316.7	13.5	72.8
Br	429.6	534.0	327.1	<i>c</i>	432.4	235.2	313.9	13.4	72.7
COOEt	442.5	530.2	311.4	13.7	442.4	239.2	294.7	12.9	74.5
NO ₂	456.1	529.6	294.1	13.5	453.9	240.1	272.5	12.5	76.1

^a The values of $\delta(\text{Se})$ and $\delta(\text{C})$ are from external MeSeMe and CDCl₃, respectively, and coupling constants are in Hz. ^b Values of $^5J(^8\text{Se}, \text{C}_{\text{Me}})$ were observed to be 15.0–16.1 Hz. ^c Not observed due to low solubility and low sensitivity.

nylselanyl)naphthyl] diselenides (1-[8-(*p*-YC₆H₄Se)C₁₀H₆]-Se-Se[C₁₀H₆(SeC₆H₄Y-*p*)-8']-1' (**1**: **1a–g** for Y = H, OMe, Me, Cl, Br, COOEt, NO₂, respectively)) were prepared by the reaction of the dianion of naphtho[1,8-*c,d*]-1,2-diselenole with 2 equiv or more of para-substituted benzenediazonium chloride at low temperature. 1-(Methylselanyl)-8-(para-substituted phenylselanyl)naphthalenes **2** (**2a–g**) were prepared by the addition of methyl iodide to aqueous THF solutions of the corresponding 8-(para-substituted phenylselanyl)-1-naphthaleneselenates, which were obtained in the reaction of **1a–g** with sodium borohydride, respectively.



	a	b	c	d	e	f	g
Y :	H	OMe	Me	Cl	Br	CO ₂ Et	NO ₂

The ^{77}Se NMR spectra of **1** and **2** are measured, along with the ^1H and ^{13}C NMR spectra for the compounds. Table 1 summarizes the ^{77}Se NMR chemical shifts and coupling constants of **1** and **2**, together with selected ^{13}C chemical shifts. The Se atoms of arylselanyl groups at the 8,8'- and 8-positions in **1** and **2** are numbered as ^8Se (or ^8Se) and other Se atoms in **1** and **2** as ^1Se (or ^1Se).

The $\delta(^8\text{Se})$ values of **1** show a good correlation with those of **2**. Figure 1 shows the results, and the correlation is shown in eq 1.^{16,17}

$$\delta(^8\text{Se}) \text{ of } \mathbf{1} = 1.33 \times \delta(^8\text{Se}) \text{ of } \mathbf{2} - 147.1 \quad (r = 0.994) \quad (1)$$

(16) The $\delta(^8\text{Se})$ values of **1** and **2** were plotted versus $\delta(\text{Se})$ of *p*-YC₆H₄SePh (**9**), and the correlations are given in eqs a and b, respectively. As shown in eqs 1, a, and b, the $\delta(^8\text{Se})$ in **1** and **2** and $\delta(\text{Se})$ in **9** are well correlated with each other, which means that the effect of the substituents on $\delta(\text{Se})$ of the *p*-YC₆H₄Se groups would be essentially the same for the three selenides, although the magnitudes of the effect are different. A slight deviation was observed for the point corresponding to Y = OMe in eq b.

$$\delta(^8\text{Se}) \text{ of } \mathbf{1} = 1.07 \times \delta(\text{Se}) \text{ of } \mathbf{9} - 21.4 \quad (r = 0.996) \quad (a)$$

$$\delta(^8\text{Se}) \text{ of } \mathbf{2} = 0.794 \times \delta(\text{Se}) \text{ of } \mathbf{9} + 98.2 \quad (r = 0.991) \quad (b)$$

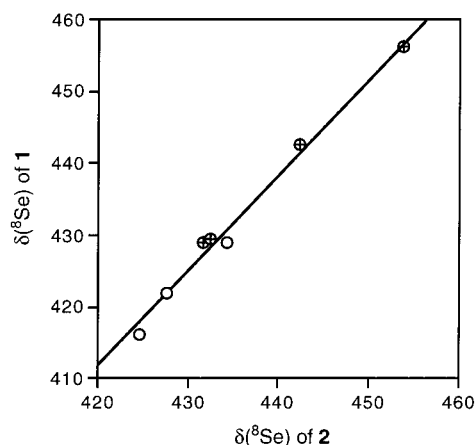


Figure 1. Plot of $\delta(^8\text{Se})$ of **1** versus $\delta(^8\text{Se})$ of **2**: O and \oplus stand for **g(m)** and **g(n)**, respectively. See also ref 20.

The substituent effect on $\delta(^8\text{Se})$ of **1** is 1.33 times larger than that of **2**. The selanyl groups at the 1-positions in **1** and **2** must affect the magnitude of the substituent effect on the $\delta(^8\text{Se})$ values relative to those of 1-(arylselanyl)naphthalenes. Therefore, the larger substituent effect for **1** may be due to the greater electron-accepting ability of the naphthyl group bearing an Se–Se bond with a low-lying $\sigma^*(\text{Se}–\text{Se})$ orbital in **1** relative to the 8-(methylselanyl)naphthyl group in **2**. The conformational effect of the ArSe group must also play an important role for the magnitude of the substituent effect. The substituent effect on the $\delta(\text{Se})$ values in *p*-YC₆H₄SeR is larger for the Se–C_R bond being in the aryl plane than for the bond perpendicular to the plane.^{18,19} The structures **1a** and **2a** correspond to the planar and the perpendicular ones, respectively.²⁰

(17) The $\delta(^8\text{Se})$ values of **1** and **2** were also plotted versus $\delta(\text{Se})$ of 1-(para-substituted phenylselanyl)naphthalenes (**10**), and the correlations are given in eqs c and d, respectively. However, the correlation for **1** (eq c) is poorer than that of eq a in ref 16. It must be due to the characteristic structures of **10**. Details will be reported elsewhere.

$$\delta(^8\text{Se}) \text{ of } \mathbf{1} = 1.51 \times \delta(\text{Se}) \text{ of } \mathbf{10} - 116.0 \quad (r = 0.987) \quad (c)$$

$$\delta(^8\text{Se}) \text{ of } \mathbf{2} = 1.14 \times \delta(\text{Se}) \text{ of } \mathbf{10} + 22.0 \quad (r = 0.997) \quad (d)$$

(18) The details of the substituent effect on $\delta(\text{Se})$ in *p*-YC₆H₄SeR (R = Me, Ph, CN, CH=CH₂ etc.), together with **1** and **2**, are discussed in ref 15. The $\delta(^8\text{Se})$ values of **1** and **2** can be discussed as a class of para-substituted phenyl selenides.

(19) Details of the substituent effect on $\delta(^8\text{Se})$ and $\delta(\text{C}_i)$ are discussed in the Supporting Information.

(20) The results show that the substituent dependence of the structures **1** and **2** would also be considered for the detail discussion, since the plot gives better correlations if it is analyzed as the two correlations with **g(m)** ($a = 1.27$ and $r = 0.990$) and **g(n)** ($a = 1.22$ and $r = 1.00$) as will be discussed in the plots of $^4J(^8\text{Se}, ^1\text{Se})$ ($= ^4J(^8\text{Se}, ^1\text{Se})$) versus $\delta(^8\text{Se})$ in **1** and **2** in the text.

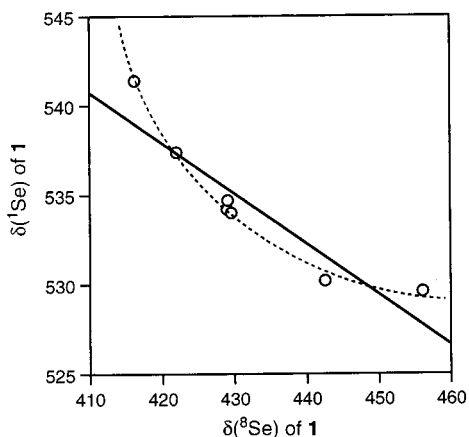


Figure 2. Plot of $\delta(^1\text{Se})$ versus $\delta(^8\text{Se})$ of **1**. Deviation from linearity is emphasized by a dotted line.

The $\delta(^1\text{Se})$ values of **1** and **2** were plotted versus $\delta(^8\text{Se})$ of **1** and **2**, respectively. Figure 2 shows the plot of $\delta(^1\text{Se})$ versus $\delta(^8\text{Se})$ of **1**, and the correlations for **1** and **2** are shown in eqs 2 and 3, respectively.

$$\delta(^1\text{Se}) \text{ of } \mathbf{1} = -0.282 \times \delta(^8\text{Se}) \text{ of } \mathbf{1} + 656.2 \quad (r = 0.924) \quad (2)$$

$$\delta(^1\text{Se}) \text{ of } \mathbf{2} = 0.252 \times \delta(^8\text{Se}) \text{ of } \mathbf{2} + 126.5 \quad (r = 0.965) \quad (3)$$

Figures 3 and 4 exhibit the plots of $^4J(^8\text{Se}, ^1\text{Se})$ ($= ^4J(^8\text{Se}, ^1\text{Se})$) versus $\delta(^8\text{Se})$ in **1** and **2**, respectively. Each plot was better analyzed as the two correlations depending on the two groups of substituents, $g(\mathbf{m})$ and $g(\mathbf{n})$: $g(\mathbf{m})$ consists of the points corresponding to $Y = \text{OMe}$, Me , and H , and the points of $Y = \text{Cl}$, Br , COEt , and NO_2 belong to $g(\mathbf{n})$. The correlations for $g(\mathbf{m})$ and $g(\mathbf{n})$ are given in eqs 4m,n and 5m,n for **1** and **2**, respectively.

$$^4J(^8\text{Se}, ^1\text{Se}) \text{ of } \mathbf{1} = -2.34 \times \delta(^8\text{Se}) \text{ of } \mathbf{1} + 1345.2 \quad (r = 0.991 \text{ for } g(\mathbf{m})) \quad (4\text{m})$$

$$^4J(^8\text{Se}, ^1\text{Se}) \text{ of } \mathbf{1} = -1.29 \times \delta(^8\text{Se}) \text{ of } \mathbf{1} + 883.5 \quad (r = 0.998 \text{ for } g(\mathbf{n})) \quad (4\text{n})$$

$$^4J(^8\text{Se}, ^1\text{Se}) \text{ of } \mathbf{2} = -1.86 \times \delta(^8\text{Se}) \text{ of } \mathbf{2} + 1128.7 \quad (r = 0.965 \text{ for } g(\mathbf{m})) \quad (5\text{m})$$

$$^4J(^8\text{Se}, ^1\text{Se}) \text{ of } \mathbf{2} = -1.96 \times \delta(^8\text{Se}) \text{ of } \mathbf{2} + 1161.0 \quad (r = 1.000 \text{ for } g(\mathbf{n})) \quad (5\text{n})$$

Figure 5 shows the plot of $^4J(^8\text{Se}, ^1\text{Se})$ of **1** versus those of **2**. The plot is also analyzed with $g(\mathbf{m})$ and $g(\mathbf{n})$, of which correlations are given in eqs 6m,n, respectively.

$$^4J(^8\text{Se}, ^1\text{Se}) \text{ of } \mathbf{1} = 1.57 \times ^4J(^8\text{Se}, ^1\text{Se}) \text{ of } \mathbf{2} - 166.3 \quad (r = 1.000 \text{ for } g(\mathbf{m})) \quad (6\text{m})$$

$$^4J(^8\text{Se}, ^1\text{Se}) \text{ of } \mathbf{1} = 0.809 \times ^4J(^8\text{Se}, ^1\text{Se}) \text{ of } \mathbf{2} + 73.4 \quad (r = 1.000 \text{ for } g(\mathbf{n})) \quad (6\text{n})$$

Now, we would like to discuss the substituent effect on $\delta(^1\text{Se})$, resulting from the nonbonded Se - - Se interac-

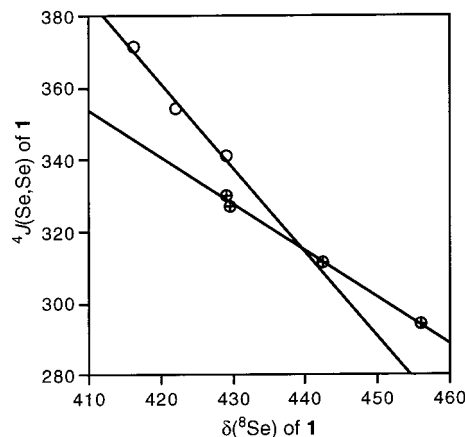


Figure 3. Plot of $^4J(\text{Se}, \text{Se})$ versus $\delta(^8\text{Se})$ of **1**: \circ and \oplus stand for $g(\mathbf{m})$ and $g(\mathbf{n})$, respectively.

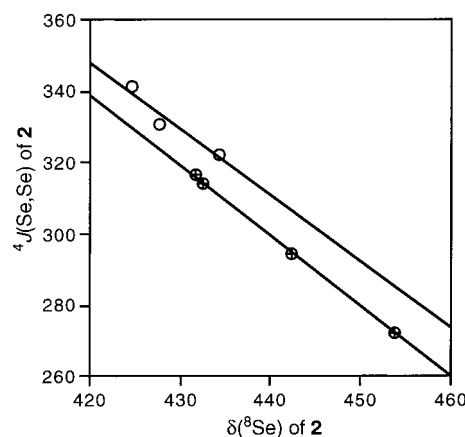


Figure 4. Plot of $^4J(\text{Se}, \text{Se})$ versus $\delta(^8\text{Se})$ of **2**: \circ and \oplus stand for $g(\mathbf{m})$ and $g(\mathbf{n})$, respectively.

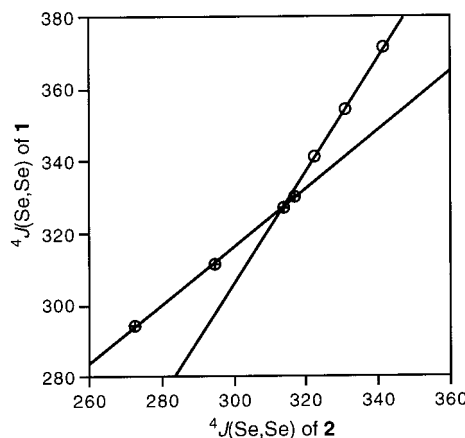


Figure 5. Plot of $^4J(\text{Se}, \text{Se})$ of **1** versus $^4J(\text{Se}, \text{Se})$ of **2**: \circ and \oplus stand for $g(\mathbf{m})$ and $g(\mathbf{n})$, respectively.

tions in **1** and **2**. As shown in Figure 2 and eq 2, the plot of $\delta(^1\text{Se})$ versus $\delta(^8\text{Se})$ in **1** gave a rather poor correlation with a negative proportionality constant (inverse correlation) so the plots had to be analyzed as inversely proportional shown by a dotted line in the Figure. On the other hand, a better correlation was held with a positive proportionality constant for **2** (regular correlation; see eq 3).

Regular correlation in **2** could be explained by assuming that the electron density on the ^1Se atom decreased as that on the ^8Se atom became smaller, if the $\delta(^8\text{Se})$ and $\delta(^1\text{Se})$ values are mainly governed by the charges on the atoms. However, there are other explanations for the regular correlation. One of mechanisms is to consider the $^1\text{Se}-\text{C}_{\text{Me}}$ bond polarization induced by the charge on the ^8Se atom. Since the electron density near the two Se atoms in **2** should be very high due to the very close location of the two Se atoms, the electrons on the Se atoms must be expelled to the adjacent atoms or the Se-C bonds. The expelled electrons from the ^1Se atom may return to the atom, if the electron density on the ^8Se atom decreased, which must result in the increase of the electron density at the ^1Se atom. The observed regular correlation in **2** can be achieved only when the $\delta(^8\text{Se})$ and $\delta(^1\text{Se})$ values shift downfield and upfield, respectively, as the charges at the Se atoms become larger, in this explanation. The contribution of the through-bond interaction must also be considered, since the π type 2c-4e orientation of the p-type lone pairs enables them to interact easily with the π -orbitals of the naphthalene ring of **2**.

The mechanism operating in the inverse correlation in **1** must be different from that of the regular correlation in **2**. It is reasonable to assume that the σ^* -orbital of the inside Se-Se bond can accept electrons of the ^8Se atoms more easily when the electron density of the ^8Se atoms increases. The electron density at the ^1Se atom will be effectively increased, as the density at the ^8Se atoms becomes larger, in this case. The NMR signals of both ^8Se and ^1Se atoms in **1** would shift in the same direction, if the chemical shifts are mainly determined by the charges on the atoms. However, the observations are just the opposite of what is expected. Therefore, the $\delta(^1\text{Se})$ values must be negatively proportional to the charges in this case. Ab initio MO calculations, containing the σ -(Se) values calculated based on the GIAO theory, will reveal the details, which will be discussed in the next section.

After establishment of the inverse correlation of $\delta(^1\text{Se})$ versus $\delta(^8\text{Se})$ in **1** experimentally, together with the regular correlation in **2**, the next extension of our study is to examine the nonbonded interaction by means of coupling constants in connection with $\delta(^8\text{Se})$ in **1** and **2**. The plot of $^4J(\text{Se},\text{Se})$ versus $\delta(^8\text{Se})$ in **1** was analyzed as two correlations as shown in Figure 3 and eqs 4m,n. The plot in **2** was similarly analyzed as the two correlations (Figure 4 and eqs 5m,n). The analysis by the two correlation methods show the importance of the substituent dependence on structures. All of the proportionality constants in eqs 4 and 5 were negative, which implies that as the value for $^4J(^8\text{Se},^1\text{Se})$ in **1** and **2** becomes smaller, then the $\delta(^8\text{Se})$ experiences a downfield shift. The results are explained well by assuming that the J values become larger as the electron density of the ^8Se atoms increases. The observation of the long-range $^5J(^8\text{Se},^1\text{Se})$ (and $^5J(^1\text{Se},^8\text{Se})$) couplings of 12–14 Hz in **1** further supports the effective orbital interaction between the ^8Se atom with the $\sigma^*(\text{Se}-\text{Se})$ orbital in **1**.

The $\delta(\text{C}_{\text{Me}})$ and $^1J(^1\text{Se},\text{C}_{\text{Me}})$ values were plotted versus those of $\delta(^8\text{Se})$ in **2**, of which correlations are given in eqs 7 and 8, respectively.

$$\delta(\text{C}_{\text{Me}}) \text{ of } \mathbf{2} = -0.048 \times \delta(^8\text{Se}) \text{ of } \mathbf{2} + 34.1 \quad (r = 0.993) \quad (7)$$

$$^1J(^1\text{Se},\text{C}_{\text{Me}}) \text{ of } \mathbf{2} = 0.154 \times \delta(^8\text{Se}) \text{ of } \mathbf{2} + 6.5 \quad (r = 0.973) \quad (8)$$

Good correlations were obtained for these plots, which demonstrated that the influence of the substituents at the phenyl para positions was transmitted even to the $\delta(\text{C}_{\text{Me}})$ and $^1J(^1\text{Se},\text{C}_{\text{Me}})$ values. These results can be explained by assuming that the fairly large interaction is operating between the lone pairs of the ^8Se atom and the $\sigma^*(^1\text{Se}-\text{C}_{\text{Me}})$ orbital. The $^8\text{Se} \cdots ^1\text{Se}-\text{C}_{\text{Me}}$ interaction can be accounted for by the contribution of the unsymmetrical 3c-4e model,²¹ as was observed in the F- \cdots -Se-C interaction.⁵ Ab initio MO calculations were performed on appropriate models of **1** and **2**, which reveal the nature of the nonbonded interactions of 4c-6e type in **1** and π type 2c-4e and/or $n(\text{Se})-\cdots\sigma^*(\text{Se}-\text{C})$ 3c-4e in **2**.

Nature of the Nonbonded Se- \cdots -Se Interactions Revealed by MO Calculations. Chart 3 shows some adducts, $p\text{-YC}_6\text{H}_4^{\text{A}}\text{SeH}-\cdots\text{BSeH}-\text{BSeH}-\cdots\text{H}^{\text{A}}\text{SeC}_6\text{H}_4\text{Y}-p$ (**3**: models of **1**) and $p\text{-YC}_6\text{H}_4^{\text{A}}\text{SeH}-\cdots\text{BSeH}_2$ (**4** and **5**: model of **2**), where the naphthylidene and methyl groups in **1** and **2** are replaced by hydrogens in the models. The structures **3**–**5** around the Se atoms are deformed but remained close to those of **1a**, **2a**, and **2d**, respectively. Ab initio molecular orbital calculations on **3**–**5** were performed with the 6-311+G(2d,p) basis sets of the Gaussian 94 program²² at the B3LYP level. Similar calculations were also performed on $p\text{-YC}_6\text{H}_4\text{SeH}$ (**6_{pl}** and **6_{pd}**),²³ where the Se-H bond is in the aryl plane in **6_{pl}** and it is perpendicular to the plane in **6_{pd}**. Ab initio MO calculations of **3**–**6** were carried out for Y = H, OH, Me, Cl, Br, COOH, and NO₂. The GIAO magnetic shielding tensor^{11,12} for the Se nucleus ($\sigma(\text{Se})$) and the natural charges (Qn) were also obtained using the natural population analysis.²⁴

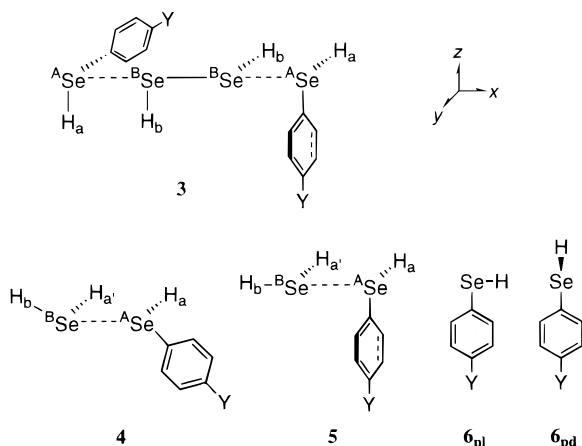
The optimized structure of **6_{pl}** was employed in **3** and **5** and **6_{pd}** in **4** without further optimization, except for $r(\text{Se}-\text{C})$, $r(\text{Se}-\text{H})$, and $\angle\text{CSeH}$, which were reoptimized in the models. As shown in Chart 3, the four Se atoms in **3** were placed on the x axis. Se-C bonds were on the y or z direction. The aryl plane was on the yz plane. Nonbonded Se- \cdots -Se distances, $r^{\text{A}}(\text{Se}-\text{BSe})$, were fixed at

(21) (a) Pimentel, G. C. *J. Chem. Phys.* **1951**, *19*, 446. Musher, J. I. *Angew. Chem., Int. Ed. Engl.* **1969**, *8*, 54. (b) Chen, M. M. L.; Hoffmann, R. *J. Am. Chem. Soc.* **1976**, *98*, 1647. (c) Cahill, P. A.; Dykstra, C. E.; Martin, J. C. *J. Am. Chem. Soc.* **1985**, *107*, 6359. See also: Hayes, R. A.; Martin, J. C. *Sulfurane Chemistry*. In *Organic Sulfur Chemistry: Theoretical and Experimental Advances*; Bernardi, F., Ciszmadia, I. G., Mangini, A., Eds.; Elsevier: Amsterdam, 1985; Chapter 8.

(22) Gaussian 94, Revision D.4: Frisch, M. J.; Trucks, G. W.; Schlegel, H. B.; Gill, P. M. W.; Johnson, B. G.; Robb, M. A.; Cheeseman, J. R.; Keith, T.; Petersson, G. A.; Montgomery, J. A.; Raghavachari, K.; Al-Laham, M. A.; Zakrzewski, V. G.; Ortiz, J. V.; Foresman, J. B.; Cioslowski, J.; Stefanov, B. B.; Nanayakkara, A.; Challacombe, M.; Peng, C. Y.; Ayala, P. Y.; Chen, W.; Wong, M. W.; Andres, J. L.; Replogle, E. S.; Gomperts, R.; Martin, R. L.; Fox, D. J.; Binkley, J. S.; Defrees, D. J.; Baker, J.; Stewart, J. P.; Head-Gordon, M.; Gonzalez, C.; Pople, J. A. Gaussian, Inc., Pittsburgh, PA, 1995.

(23) The structures **6_{pl}** and **6_{pd}** (a-g for Y = H, OH, Me, Cl, Br, COOH, and NO₂, respectively) were fully optimized with the 6-311+G-(2d,p) basis sets at the B3LYP level except for **6_{pd}** with Y = COOH. Calculations for **6_{pd}** with Y = COOH were achieved with the torsional angle between the Se-H bond and the phenyl plane fixed to be perpendicular. The structures **6_{pl}** and **6_{pd}** would not be the energy minima but the transition states.^{15b}

(24) NBO Ver. 3.1: Glendening, E. D.; Reed, A. E.; Carpenter, J. E.; Weinhold, F.

Chart 3. Structures of Models 3–6, Together with the Axes**Table 2. Results of ab Initio MO Calculations on 3 with the 6-311+G(2d,p) Basis Sets^{a,b}**

Y	Qn(^A Se) _B ^c	Qn(^B Se) _B ^c	δ (^A Se) _B ^d	δ (^B Se) _B ^d	δ (^A Se) _H ^e	δ (^B Se) _H ^e
OH	0.2075	-0.1686	108.26	-28.99	132.15	2.32
Me	0.2107	-0.1670	112.13	-28.71	137.11	1.98
H	0.2137	-0.1665	120.26	-28.77	145.92	1.41
Cl	0.2239	-0.1657	120.50	-28.07	148.59	1.08
Br	0.2231	-0.1657	120.50	-28.06	149.79	0.89
CO-	0.2315	-0.1640	<i>f</i>	<i>f</i>	165.60	-1.54
OH						
NO ₂	0.2460	-0.1620	149.10	-24.46	175.21	-2.09

^aThe $\sigma(\text{Se})$ values for MeSeMe are 1645.53 and 1915.42 with B3LYP/6-311+G(2d,p) and HF/6-311+G(2d,p)//B3LYP/6-311+G(2d,p) methods, respectively. ^bSubscripts B and H show B3LYP and HF levels, respectively. ^cCalculated with the B3LYP/3-21G*/B3LYP/6-311+G(2d,p) method. ^dCalculated with the B3LYP/6-311+G(2d,p) method. ^eCalculated with the HF/6-311+G(2d,p)//B3LYP/6-311+G(2d,p) method. ^fNot obtained due to "consistency failure" in the calculations.

the observed value of 3.053 Å in **1a**. The two ^BSe–H_b bonds of the central H₂Se₂ component were placed on the *xz* and *xy* planes. The $r(\text{Se}–\text{H})$, $r(\text{Se}–\text{C})$, $r(\text{Se}–\text{Se})$, $\angle\text{C}^{\text{A}}\text{SeH}_a$, and $\angle\text{B}^{\text{B}}\text{Se}^{\text{B}}\text{SeH}_b$ were optimized. The arylselanyl group and the ^BSe and H_b atoms in **4** were placed on the *xz* plane. The $\angle\text{C}^{\text{A}}\text{Se}^{\text{B}}\text{Se}$ and $\angle\text{A}^{\text{A}}\text{Se}^{\text{B}}\text{SeH}_b$ were fixed at the observed values of 157.0° and 144.4°, respectively, and the nonbonded Se–Se distance ($r(\text{A}^{\text{A}}\text{Se}–\text{B}^{\text{B}}\text{Se})$) was fixed at the observed value of 3.070 Å in **2a**. Two other Se–H bonds were in the plane perpendicular to the *xz* plane, and the $r(\text{Se}–\text{H})$, $r(\text{Se}–\text{C})$, $\angle\text{CSeH}$, and $\angle\text{HSeH}$ were optimized. The components of **5**, *p*-YC₆H₄SeH and HSeH, were located in the *yz* and *xy* planes, respectively, with the C–Se and Se–Se–H bonds on the *z* and *x* axes.

The nonbonded Se–Se distance ($r(\text{A}^{\text{A}}\text{Se}–\text{B}^{\text{B}}\text{Se})$) was also fixed at 3.070 Å. The $r(\text{Se}–\text{H})$, $r(\text{C}–\text{Se})$, $\angle\text{CSeH}$, and $\angle\text{HSeH}$ were optimized.

Structures **3** were optimized in the limited conditions with the B3LYP/6-311+G(2d,p) method. The natural population analysis could not be achieved with the method due to the "strongly delocalized NBO set" in the calculations; therefore, natural charges were obtained with the B3LYP/3-21G* method, using the structures obtained by the B3LYP/6-311+G(2d,p) method. The $\sigma(\text{Se})$ value of **3f** was not obtained by the B3LYP/6-311+G(2d,p) method due to "consistency failure" in the calculations. Thus, the $\sigma(\text{Se})$ values of **3** were calculated with the 6-311+G(2d,p) basis sets at the Hartree–Fock (HF) level. Table 2 exhibits the results of MO calculations for **3** where the $\sigma(\text{Se})$ values are given by the calculated $\delta(\text{Se})$ values, which are defined as $-(\sigma(\text{Se}) - \sigma(\text{Se})_{\text{MeSeMe}})$. Structures **4** and **5** were also optimized in the limited conditions with the B3LYP/6-311+G(2d,p) method. While the Qn and $\sigma(\text{Se})$ values for **5** were obtained with the method, the $\sigma(\text{Se})$ values for **4f** and **4g** could not be obtained by the method. Therefore, the $\sigma(\text{Se})$ values of **4** were recalculated with the HF/6-311+G(2d,p) method. Table 3 summarizes the results obtained for **4** and **5**. Correlations between the calculated values in **3–5** are summarized in Table 4.

Let us discuss the characteristics of the interaction of 4c–6e in **3** first, based on the results of ab initio MO calculations shown in Table 4 (nos. 1–7). The Qn(^BSe)_B values correlate well with those of Qn(^ASe)_B, where the subscript B stands for the B3LYP level. The results further show that the magnitude of the charge transfer from ^ASe to ^BSe in **3** becomes greater as the electron density on ^ASe increases, which must be a reflection of the $n(\text{A}^{\text{A}}\text{Se}) - \sigma^*(\text{B}^{\text{B}}\text{Se}–\text{B}^{\text{B}}\text{Se}) - n(\text{A}^{\text{A}}\text{Se})$ -type interaction of the bond. While $\delta(\text{B}^{\text{B}}\text{Se})_B$ correlated with $\delta(\text{A}^{\text{A}}\text{Se})_B$ accompanied by a positive proportionality constant of 0.115, the proportionality constant was -0.111 in the correlation between $\delta(\text{B}^{\text{B}}\text{Se})_H$ and $\delta(\text{A}^{\text{A}}\text{Se})_H$, where the subscript H means the HF level. Computation at the B3LYP level could not explain the observed values. This discrepancy arises from the positive proportionality constant in the correlation of $\delta(\text{B}^{\text{B}}\text{Se})_B$ versus Qn(^BSe)_B (no. 3). The value is negative in the correlation of $\delta(\text{B}^{\text{B}}\text{Se})_H$ with Qn(^BSe)_B (no. 6). The calculations at the B3LYP level usually explain the observed values better than those at the HF level.^{14,15} However, the results at the HF level reproduced the observed substituent effect on $\delta(\text{Se})$ of **1** but those at the B3LYP level did not, in this case. The superior nature of the calculations at the DFT (B3LYP) level comes from

Table 3. Results of ab Initio MO Calculations on 4 and 5 with the B3LYP/6-311+G(2d,p) Method^{a,b}

Y	4									5					
	Qn(^A Se)	Qn(^B Se)	Qn(H _b)	δ (^A Se)	δ (^B Se)	δ (H _b)	δ (^A Se) ^c	δ (^B Se) ^c	δ (H _b) ^c	Qn(^A Se)	Qn(^B Se)	Qn(H _b)	δ (^A Se)	δ (^B Se)	δ (H _b)
OH	0.0882	-0.1669	0.0816	30.56	-400.01	1.769	77.59	-239.53	2.103	0.1704	-0.2022	0.0572	104.79	-389.24	2.055
Me	0.0855	-0.1669	0.0814	37.59	-399.56	1.783	83.20	-239.09	2.109	0.1731	-0.2013	0.0573	108.48	-389.23	2.044
H	0.0861	-0.1668	0.0821	49.99	-398.76	1.801	92.75	-238.71	2.130	0.1776	-0.2019	0.0586	115.35	-387.28	2.071
Cl	0.0923	-0.1671	0.0844	39.47	-398.34	1.809	88.36	-238.78	2.153	0.1857	-0.2037	0.0615	118.21	-386.56	2.092
Br	0.0926	-0.1671	0.0845	39.70	-397.96	1.812	89.28	-238.47	2.157	0.1869	-0.2038	0.0618	117.89	-386.18	2.095
CO-	0.0924	-0.1669	0.0850	<i>d</i>	<i>d</i>	<i>d</i>	99.30	-238.04	2.180	0.1998	-0.2045	0.0639	137.43	-385.84	2.094
OH															
NO ₂	0.0994	-0.1672	0.0881	<i>d</i>	<i>d</i>	<i>d</i>	102.05	-239.38	2.227	0.2154	-0.2065	0.0683	150.20	-384.20	2.130

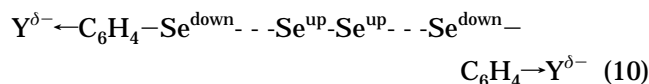
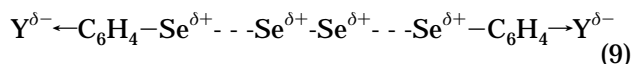
^aThe $\sigma(\text{Se})$ values for MeSeMe are 1645.53 and 1915.42 with B3LYP/6-311+G(2d,p) and HF/6-311+G(2d,p)//B3LYP/6-311+G(2d,p) methods, respectively. ^bThe $\sigma(\text{H})$ values for TMS are 31.945 and 32.198 with B3LYP/6-311+G(2d,p) and HF/6-311+G(2d,p)//B3LYP/6-311+G(2d,p) methods, respectively. ^cCalculated with the HF/6-311+G(2d,p)//B3LYP/6-311+G(2d,p) method. ^dNot obtained due to "consistency failure" in the calculations.

Table 4. Correlations between Calculated Values for 3–5^{a,b}

no.	Y	X	a	b	r	n
1	Qn(^B Se) _B of 3	Qn(^A Se) _B of 3	0.156	-0.2004	0.981	7
2	δ(^A Se) _B of 3	Qn(^A Se) _B of 3	990.2	-96.85	0.967	6 ^c
3	δ(^B Se) _B of 3	Qn(^B Se) _B of 3	733.5	93.85	0.948	6 ^c
4	δ(^B Se) _B of 3	δ(^A Se) _B of 3	0.115	-41.86	0.970	6 ^c
5	δ(^A Se) _H of 3	Qn(^A Se) _B of 3	1102.2	-94.45	0.974	7
6	δ(^B Se) _H of 3	Qn(^B Se) _B of 3	-769.8	-126.93	0.957	7
7	δ(^B Se) _H of 3	δ(^A Se) _H of 3	-0.111	17.35	0.985	7
8	Qn(^B Se) _B of 4	Qn(^A Se) _B of 4	-0.026	-0.1646	0.860	7
9	Qn(^H b) _B of 4	Qn(^A Se) _B of 4	0.486	0.0397	0.978	7
10	δ(^A Se) _H of 4	Qn(^A Se) _B of 4	1223.2	-20.87	0.686	7
11	δ(^B Se) _H of 4	Qn(^B Se) _B of 4	612.2	-136.62	0.172	7
12	δ(^H b) _H of 4	Qn(^H b) _B of 4	17.79	0.659	0.985	7
13	δ(^B Se) _H of 4	δ(^A Se) _H of 4	0.025	-241.15	0.419	7
14	δ(^H b) _H of 4	δ(^A Se) _H of 4	0.0045	1.742	0.901	7
15	Qn(^B Se) _B of 5	Qn(^A Se) _B of 5	-0.108	-0.1833	0.963	7
16	Qn(^H b) _B of 5	Qn(^A Se) _B of 5	0.249	0.0147	0.993	7
17	δ(^A Se) _B of 5	Qn(^A Se) _B of 5	1006.9	-66.52	0.988	7
18	δ(^B Se) _B of 5	Qn(^B Se) _B of 5	-949.5	-580.07	0.928	7
19	δ(^H b) _B of 5	Qn(^H b) _B of 5	6.968	1.656	0.965	7
20	δ(^B Se) _B of 5	δ(^A Se) _B of 5	0.102	-399.40	0.910	7
21	δ(^H b) _B of 5	δ(^A Se) _B of 5	0.0016	1.891	0.889	7

^a Y = aX + b (r: correlation coefficient). ^b Subscripts B and H show B3LYP and HF levels, respectively. ^c Without the point for Y = COOH.

inclusion of the electron correlation effect in the calculations, but the method sometimes overestimates this effect.¹⁴ This overestimation of the electron correlation effect at the B3LYP level might lead to failure. The characters in the substituent effect on the atomic charges and the δ(Se) values of **3** are shown in eqs 9 and 10, respectively, assuming Y is electron withdrawing. The superscript up (or down) in eq 10 shows upfield (or downfield) shifts in the δ(Se) values.



The correlations in **4** are shown in Table 4 (nos. 8–14), which are mainly the results of the HF level. The p-type lone pairs of the Se atoms in **2a** can interact through π orbitals of the naphthalene ring, as was shown in the sulfur analogue. The mechanism of the substituent effect on δ(¹Se) in **2** would be through-bond by way of the naphthylidene π-system, if the structures **2** are very close to that of **2a**. The results of the calculations on **4** are in accordance of the expectation. Nevertheless, the ^BSe–H_b polarization mechanism is predicted to operate in **4**.

Correlations with **5** exhibit the typical characters expected for the ^ASe– -^BSe–H_b 3c-4e type interaction (Table 4, nos. 15–21). The observed δ(Se) values in **2** can be well explained by the results of the calculations on **5** at least in a qualitative sense. The proportionality constant of no. 20 in Table 4 (0.102) is smaller than that of eq 3 (0.252), which may be due to the contribution of a mechanism other than **5** such as the through-bond mechanism discussed above. We believe that the mechanism shown for **5** is substantially the same as that operating in **2d–g**. This mechanism may also be operating in **2a–c**, as well as a through-bond mechanism. The nature of the substituent effect on the atomic charges and the δ(Se) values are shown in eqs 11 and 12,

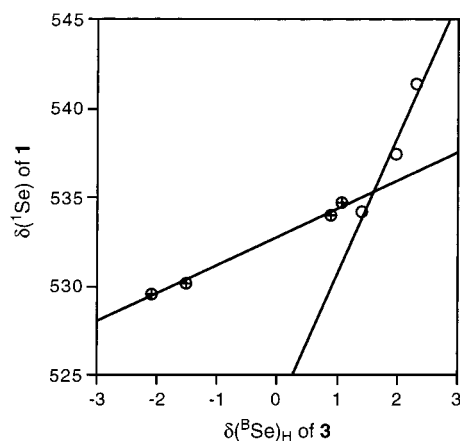
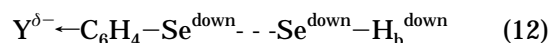
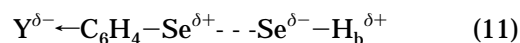
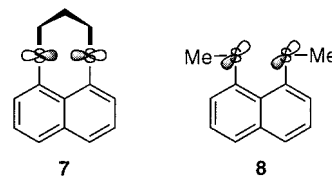


Figure 6. Plot of δ(¹Se) of **1** versus δ(^BSe)_H of **3**: ○ and □ stand for g(m) and g(n), respectively.

respectively,



exemplified by the electron-withdrawing group of Y. The δ(C_{Me}) values in **2** go upfield when Y = electron-withdrawing, which is just the opposite of that predicted for H_b shown in eq 12. The discrepancy may arise from the difference between H in **5** and CH₃ in **2**: the C–H bond in **2** can also be polarized.



Glass and co-workers have shown that the p-type lone pairs of sulfur atoms in naphtho[1,8-*b,c*]-1,5-dithiocin (**7**) lie in the naphthyl plane and interact directly with each other, whereas those in 1,8-bis(methylthio)naphthalene (**8**) mainly interact with the π-orbitals of the naphthalene ring.⁸ The orientation of the lone pairs of Se atoms in PhSe groups of **1a** is close to that in the S atoms of the former, whereas that of the Se atoms in **2a** is very similar to that in S atoms of the latter. The role of the π-framework must be important in the transmittance of the substituent effect in **2** as discussed in **4**.

The Correlation of Observed and Calculated Values. The observed NMR parameters are plotted versus the calculated ones. The correlations of δ(⁸Se) of **1** versus δ(^ASe)_B and δ(^ASe)_H in **3** are shown in eqs 13 and 14, respectively. The *a* and *r* values in eq 13 are very close to 1.0, which suggests that **3** can be a good model of **1**, as a first approximation. The δ(¹Se) values of **1** are plotted versus δ(^BSe)_H of **3**. The plot is shown in Figure 6 and is analyzed as two correlations with g(m) and g(n), which are shown in eqs 15m and 15n, respectively. The necessity of needing two correlations may be due to the conformational effects of the phenyl group in **1** (see also Chart 1). A plot of δ(⁸Se) of **2** versus δ(^ASe)_B of **5** is similarly analyzed by the two correlation methods, which are shown in eqs 16m and 16n, respectively. The results

suggest the contribution of mechanism **5** for the transmittance of substituent effects in **2**.

$$\delta(^8\text{Se}) \text{ of } \mathbf{1} = 0.953 \times \delta(^A\text{Se})_B \text{ of } \mathbf{3} + 314.2 \quad (r = 0.999) \quad (13)$$

$$\delta(^8\text{Se}) \text{ of } \mathbf{1} = 0.869 \times \delta(^A\text{Se})_H \text{ of } \mathbf{3} + 301.2 \quad (r = 0.990) \quad (14)$$

$$\delta(^1\text{Se}) \text{ of } \mathbf{1} = 7.675 \times \delta(^B\text{Se})_H \text{ of } \mathbf{3} + 523.1 \quad (r = 0.978 \text{ for } g(\mathbf{m})) \quad (15m)$$

$$\delta(^1\text{Se}) \text{ of } \mathbf{1} = 1.585 \times \delta(^B\text{Se})_H \text{ of } \mathbf{3} + 532.8 \quad (r = 0.997 \text{ for } g(\mathbf{n})) \quad (15n)$$

$$\delta(^8\text{Se}) \text{ of } \mathbf{2} = 0.932 \times \delta(^A\text{Se})_B \text{ of } \mathbf{5} + 326.7 \quad (r = 1.000 \text{ for } g(\mathbf{m})) \quad (16m)$$

$$\delta(^8\text{Se}) \text{ of } \mathbf{2} = 0.657 \times \delta(^A\text{Se})_B \text{ of } \mathbf{5} + 354.1 \quad (r = 0.991 \text{ for } g(\mathbf{n})) \quad (16n)$$

We would like to comment on the $^4J(^8\text{Se}, ^1\text{Se})$ values of **1** and **2** next, although the J values were not calculated. The $^4J(^8\text{Se}, ^1\text{Se})$ values of **1** and **2** are plotted versus $Q_n(^A\text{Se})_B$ of **3** and **5**, respectively, of which correlations are given in eqs 17 and 18. The negative proportionality constants in eqs 17 and 18 clearly show that the J values become larger if the electron density on the ^ASe atoms increases, as suggested in the previous section. The correlation coefficient of eq 17 is smaller than that of eq 18.

$$^4J(^8\text{Se}, ^1\text{Se}) \text{ of } \mathbf{1} = -1877 \times Q_n(^A\text{Se})_B \text{ of } \mathbf{3} + 750.2 \quad (r = 0.969) \quad (17)$$

$$^4J(^8\text{Se}, ^1\text{Se}) \text{ of } \mathbf{2} = -1439 \times Q_n(^A\text{Se})_B \text{ of } \mathbf{5} + 582.4 \quad (r = 0.993) \quad (18)$$

Although there are some common terms in the equations for the $\delta(\text{Se})^{25}$ and $J(\text{Se}, \text{Se})^{26}$ values, one must be careful when the mechanism of the nuclear couplings is considered in relation to the chemical shifts. The contribution of the 4s-orbitals of the Se atoms to $J(\text{Se}, \text{Se})^{27,28}$ is in striking contrast to the significant contribution of the 4p atomic orbitals to the diamagnetic term of the $\delta(\text{Se})$ values. A through-space mechanism must be operating for the nonbonded Se - - Se nuclear spin-spin couplings, even if the substituent effect on the remote atomic charges is effectively transmitted through the π -framework as expected in **2** and which is missing in **4** and **5**.²⁹ The correlations of the Q_n , $\delta(\text{Se})$, with the J values for **1** show that this effect is transmitted by a through-space mechanism in contrast to the situation in **2**. The mechanism for **2** would change from mainly **4** for $g(\mathbf{m})$ to mainly **5** for $g(\mathbf{n})$. Analysis of the two correlations for the

plot of $^4J(^8\text{Se}, ^1\text{Se})$ of **1** versus those of **2** (eqs 6m,n) may shed light on the situation discussed above.

Further study on the nonbonded interactions containing the Se atom(s) is currently in progress.

Experimental Section

Chemicals were used without further purification unless otherwise noted. Solvents were purified by standard methods. Melting points were uncorrected. ^1H , ^{13}C , and ^{77}Se NMR spectra were measured at 400, 100, and 76 MHz, respectively, with a JEOL JNM-LA 400 spectrometer. The ^1H , ^{13}C , and ^{77}Se chemical shifts are given in ppm relative to those of internal CHCl_3 slightly contaminated in the solution, CDCl_3 as the solvent, and external MeSeMe , respectively. Column chromatography was performed on silica gel (Fuji Silysia BW-300), acidic alumina and basic alumina (E. Merk).

Preparation. The diselenide **1a**¹ and the bis-selenide **2a**¹ were prepared by the same method as shown in the previous paper. The selenides *p*- $\text{YC}_6\text{H}_4\text{SePh}$ (**9**) were prepared similarly to the method shown in the literature.^{15b,30,31} The reaction of *p*-iodonitrobenzene with sodium benzeneselenate in ethanol was more effective to prepare **9g**.

1a: mp 162–163 °C (lit.¹ mp 161–163 °C). **2a:** mp 101.5–102.5 °C (lit.¹ mp 101.5–102.5 °C). **9b:** mp 45–46 °C (lit.³⁰ mp 45–46 °C). **9c:** colorless oil; bp 100–101 °C/1 mmHg (lit.³⁰ bp 100 °C/1 mmHg). **9d:** colorless oil; bp 148–149 °C/1 mmHg (lit.³⁰ bp 145–150 °C/1 mmHg). **9e:** mp 32–33 °C (lit.³⁰ mp 32 °C). **9f:** colorless oil.^{15b} **9g:** mp 58–59 °C (lit.^{15b,31} mp 58 °C).

Bis[8-(*p*-methoxyphenylselanyl)naphthyl]-1,1'-diselenide (1b**).** To a solution of the dianion of naphtho[1,8-*c,d*]-1,2-diselenole, which was prepared by reduction of the diselenole with NaBH_4 in an aqueous THF, was added *p*-methoxybenzenediazonium chloride at low temperature. After usual workup, the solution was chromatographed on silica gel containing acidic and basic alumina. Recrystallization of the chromatographed product from hexane gave **1b** as a yellow solid: 69% yield; mp 143.5–145.0 °C; ^1H NMR (CDCl_3 , 400 MHz) 3.74 (s, 6H), 6.75 (dd, 4H, $J = 8.9, 2.6$ Hz), 7.18 (t, 2H, $J = 7.8$ Hz), 7.32 (t, 2H, $J = 7.6$ Hz), 7.32 (dd, 4H, $J = 9.0, 2.7$ Hz), 7.67 (dd, 2H, $J = 8.0, 0.9$ Hz), 7.79 (dd, 2H, $J = 8.1, 1.0$ Hz), 7.86 (dd, 2H, $J = 7.2, 1.4$ Hz), 8.14 (dd, 2H, $J = 7.5, 1.0$ Hz); ^{13}C NMR (CDCl_3 , 100 MHz) 55.27, 115.06, 125.28, 125.82, 126.52, 128.33, 129.78, 130.25, 130.57, 132.74, 133.42, 135.39, 136.14, 137.39, 159.24; ^{77}Se NMR (CDCl_3 , 76 MHz) 416.2, 541.4 ($^4J(^8\text{Se}, ^1\text{Se}) = 371.6$ Hz). Anal. Calcd for $\text{C}_{34}\text{H}_{26}\text{O}_2\text{Se}_4$: C, 52.19; H, 3.35. Found: C, 52.45; H, 3.36.

Bis[8-(*p*-methylphenylselanyl)naphthyl]-1,1'-diselenide (1c**).** Following a method similar to that for **1b**, **1c** gave 72% yield as a yellow solid: mp 165.5–166.5 °C; ^1H NMR (CDCl_3 , 400 MHz) 2.27 (s, 6H), 7.00 (dd, 4H, $J = 8.3, 2.5$ Hz), 7.16 (t, 2H, $J = 7.8$ Hz), 7.20 (dd, 4H, $J = 8.2, 2.5$ Hz), 7.34 (t, 2H, $J = 7.9$ Hz), 7.67 (dd, 2H, $J = 8.1, 0.8$ Hz), 7.83 (dd, 2H, $J = 8.2, 1.2$ Hz), 7.92 (dd, 2H, $J = 7.2, 1.3$ Hz), 8.11 (dd, 2H, $J = 7.5, 1.0$ Hz); ^{13}C NMR (CDCl_3 , 100 MHz) 21.06, 125.84, 126.57, 128.16, 128.40, 130.09, 130.49, 130.66, 130.86, 131.68, 132.32, 135.62, 136.15, 136.79, 138.37; ^{77}Se NMR (CDCl_3 , 76 MHz) 422.0, 537.4 ($^4J(^8\text{Se}, ^1\text{Se}) = 354.4$ Hz). Anal. Calcd for $\text{C}_{34}\text{H}_{26}\text{Se}_4$: C, 54.42; H, 3.49. Found: C, 54.71; H, 3.57.

Bis[8-(*p*-chlorophenylselanyl)naphthyl]-1,1'-diselenide (1d**).** Following a method similar to that for **1b**, **1d** gave 68% yield as a yellow solid: mp 185.0–186.0 °C; ^1H NMR (CDCl_3 , 400 MHz) 7.13 (br s, 8H), 7.16 (t, 2H, $J = 7.8$ Hz), 7.38 (t, 2H, $J = 7.7$ Hz), 7.70 (dd, 2H, $J = 8.0, 0.8$ Hz), 7.88 (dd, 2H, $J = 8.2, 1.1$ Hz), 7.94 (dd, 2H, $J = 7.2, 1.3$ Hz), 8.02 (dd, 2H, $J = 7.5, 1.1$ Hz); ^{13}C NMR (CDCl_3 , 100 MHz) 125.95, 126.75, 127.26, 128.43, 129.42, 130.19, 131.28, 131.65, 132.48, 132.91, 133.82, 135.62, 136.36, 139.01; ^{77}Se NMR (CDCl_3 , 76

(25) Karplus, M.; Pople, J. A. *J. Chem. Phys.* **1963**, *38*, 2803.

(26) McConnell, H. M., *J. Chem. Phys.* **1956**, *24*, 460.

(27) Reich, H. J.; Trend, J. E. *J. Chem. Soc., Chem. Commun.* **1976**, 310.

(28) Nakanishi, W.; Ikeda, Y. *Bull. Chem. Soc. Jpn.* **1983**, *56*, 1161.

(29) The contribution of the through-bond mechanism is estimated to be very small for $^4J(\text{F}, \text{F})$ in 1,8-di(fluoro)naphthalene.^{6b}

(30) Greenberg, B.; Gold, E. S.; Burlant, W. M. *J. Am. Chem. Soc.* **1956**, *78*, 4028.

(31) *Chem. Abstr.* **1955**, *49*, 2349g.

MHz) 429.1, 534.7 ($^4J^{8}\text{Se}, ^1\text{Se}$) = 330.1 Hz). Anal. Calcd for $\text{C}_{32}\text{H}_{20}\text{Se}_4\text{Cl}_2$: C, 48.58; H, 2.55. Found: C, 48.77; H, 2.56.

Bis[8-(*p*-bromophenylselanyl)naphthyl]-1,1'-diselenide (1e). Following a method similar to that for **1b**, **1e** gave 72% yield as a yellow solid: mp 203.0–205.0 °C; ^1H NMR (CDCl_3 , 400 MHz) 7.06 (dd, 4H, J = 6.6, 2.2 Hz), 7.16 (t, 2H, J = 7.8 Hz), 7.27 (dd, 4H, J = 8.6, 2.2 Hz), 7.38 (t, 2H, J = 7.6 Hz), 7.70 (dd, 2H, J = 8.1, 0.9 Hz), 7.89 (dd, 2H, J = 8.2, 1.2 Hz), 7.95 (dd, 2H, J = 7.1, 1.3 Hz), 8.01 (dd, 2H, J = 7.5, 1.1 Hz); ^{13}C NMR (CDCl_3 , 100 MHz) 120.77, 125.95, 126.78, 126.85, 128.40, 130.02, 131.38, 131.71, 132.28, 132.29, 134.56, 135.54, 136.32, 139.19; ^{77}Se NMR (CDCl_3 , 76 MHz) 429.6, 534.0 ($^4J^{8}\text{Se}, ^1\text{Se}$) = 327.1 Hz). Anal. Calcd for $\text{C}_{32}\text{H}_{20}\text{Se}_4\text{Br}_2$: C, 43.67; H, 2.29. Found: C, 43.84; H, 2.25.

Bis[8-[*p*-(ethoxycarbonyl)phenylselanyl]naphthyl]-1,1'-diselenide (1f). Following a method similar to that for **1b**, **1f** gave 58% yield as a yellow solid: mp 167.0–169.5 °C; ^1H NMR (CDCl_3 , 400 MHz) 1.34 (t, 6H, J = 7.1 Hz), 4.32 (q, 4H, J = 7.1 Hz), 7.12 (t, 2H, J = 7.8 Hz), 7.15 (dd, 2H, J = 8.7, 1.9 Hz), 7.39 (t, 2H, J = 7.6 Hz), 7.67 (dd, 2H, J = 8.0, 0.9 Hz), 7.81 (dd, 4H, J = 8.6, 1.9 Hz), 7.90 (dd, 2H, J = 8.2, 1.1 Hz), 7.97 (dd, 2H, J = 7.6, 1.2 Hz), 7.98 (dd, 2H, J = 7.1, 1.4 Hz); ^{13}C NMR (CDCl_3 , 100 MHz) 14.28, 60.83, 125.64, 125.93, 126.79, 128.27, 128.34, 128.78, 129.90, 130.13, 131.71, 132.07, 135.70, 136.36, 139.80, 142.50, 166.17; ^{77}Se NMR (CDCl_3 , 76 MHz) 442.5, 530.2 ($^4J^{8}\text{Se}, ^1\text{Se}$) = 311.4 Hz). Anal. Calcd for $\text{C}_{38}\text{H}_{30}\text{Se}_4\text{O}_4$: C, 52.67; H, 3.49. Found: C, 52.84; H, 3.50.

Bis[8-(*p*-nitrophenylselanyl)naphthyl]-1,1'-diselenide (1g). Following a method similar to that for **1b**, **1g** gave 56% yield as a yellow solid: mp 230.0–233.5 °C; ^1H NMR (CDCl_3 , 400 MHz) 7.14 (t, 2H, J = 7.8 Hz), 7.16 (dd, 2H, J = 9.0, 2.5 Hz), 7.46 (t, 2H, J = 7.7 Hz), 7.73 (dd, 2H, J = 8.1, 1.0 Hz), 7.91 (dd, 2H, J = 7.6, 1.1 Hz), 7.97 (dd, 4H, J = 9.0, 2.2 Hz), 7.99 (dd, 2H, J = 7.9, 1.3 Hz), 8.02 (dd, 2H, J = 7.1, 1.4 Hz); ^{13}C NMR (CDCl_3 , 100 MHz) 124.10, 124.42, 126.22, 126.97, 128.66, 128.84, 129.45, 132.11, 132.48, 135.55, 136.56, 140.34, 146.00, 146.15; ^{77}Se NMR (CDCl_3 , 76 MHz) 456.1, 529.6 ($^4J^{8}\text{Se}, ^1\text{Se}$) = 294.1 Hz). Anal. Calcd for $\text{C}_{32}\text{H}_{20}\text{Se}_4\text{N}_2\text{O}_4$: C, 47.31; H, 2.48; N, 3.45. Found: C, 47.52; H, 2.58; N, 3.35.

1-(Methylselanyl)-8-(*p*-methoxyphenylselanyl)naphthalene (2b). The diselenide **1b** was reduced by NaBH_4 in aqueous THF and then allowed to react with methyl iodide to give **2b** as a white solid: 91% yield; mp 86.0–87.0 °C; ^1H NMR (CDCl_3 , 400 MHz) 2.38 (s, 3H, $J(\text{Se}, \text{H})$ = 13.4 Hz), 3.79 (s, 3H), 6.83 (dd, 2H, J = 8.6, 2.2 Hz), 7.17 (t, 1H, J = 7.7 Hz), 7.33 (t, 1H, J = 7.7 Hz), 7.45 (dd, 2H, J = 8.1, 2.2 Hz), 7.45 (dd, 1H, J = 6.8, 1.1 Hz), 7.64 (dd, 1H, J = 8.1, 1.0 Hz), 7.70 (dd, 1H, J = 8.0, 1.1 Hz), 7.79 (dd, 1H, J = 7.3, 1.1 Hz); ^{13}C NMR (CDCl_3 , 100 MHz) 13.90 (1J = 71.2 Hz, 5J = 15.7 Hz), 55.23, 115.17, 124.73, 125.70, 125.84, 128.26, 128.75, 131.25, 133.10, 133.50, 133.64, 134.94, 135.80, 136.47 (1J = 11.5 Hz), 159.69; ^{77}Se NMR (CDCl_3 , 76 MHz) 424.5, 233.1 ($^4J^{8}\text{Se}, ^1\text{Se}$) = 341.6 Hz). Anal. Calcd for $\text{C}_{18}\text{H}_{16}\text{Se}_2\text{O}$: C, 53.22; H, 3.97. Found: C, 53.35; H, 3.90.

1-(Methylselanyl)-8-(*p*-methylphenylselanyl)naphthalene (2c). Following a method similar to that for **2b**, **2c** gave 89% yield as a white solid: mp 78.5–79.5 °C; ^1H NMR (CDCl_3 , 400 MHz) 2.32 (s, 3H), 2.36 (s, 3H, $J(\text{Se}, \text{H})$ = 13.9 Hz), 7.08 (dd, 2H, J = 7.8, 2.2 Hz), 7.20 (t, 1H, J = 7.7 Hz), 7.34 (t, 1H, J = 7.8 Hz), 7.36 (dd, 2H, J = 8.0, 2.2 Hz), 7.58 (dd, 1H, J = 7.5, 1.3 Hz), 7.69 (dd, 1H, J = 8.2, 1.1 Hz), 7.71 (dd, 1H, J = 8.4, 1.1 Hz), 7.76 (dd, 1H, J = 7.4, 1.3 Hz); ^{13}C NMR (CDCl_3 , 100 MHz) 13.65 (1J = 72.8 Hz, 5J = 16.6 Hz), 21.27, 125.77, 125.88, 128.46, 128.77, 130.22, 131.24, 131.74, 132.22, 132.79, 133.86 (1J = 11.6 Hz), 134.52, 135.17, 135.78, 137.53; ^{77}Se NMR (CDCl_3 , 76 MHz) 427.7, 234.5 ($^4J^{8}\text{Se}, ^1\text{Se}$) = 330.9 Hz). Anal. Calcd for $\text{C}_{18}\text{H}_{16}\text{Se}_2$: C, 55.40; H, 4.13. Found: C, 55.52; H, 4.19.

1-(Methylselanyl)-8-(*p*-chlorophenylselanyl)naphthalene (2d). Following a method similar to that for **2b**, **2d** gave 87% yield as a white solid: mp 78.5–79.5 °C; ^1H NMR (CDCl_3 , 400 MHz) 2.34 (s, 3H, $J(\text{Se}, \text{H})$ = 13.9 Hz), 7.19 (dd, 2H, J =

8.6, 2.2 Hz), 7.24 (t, 1H, J = 7.7 Hz), 7.31 (dd, 2H, J = 8.8, 2.2 Hz), 7.36 (t, 1H, J = 7.7 Hz), 7.60 (dd, 1H, J = 7.3, 1.5 Hz), 7.71 (dd, 1H, J = 7.1, 1.2 Hz), 7.73 (dd, 1H, J = 6.8, 1.1 Hz), 7.74 (dd, 1H, J = 7.3, 1.2 Hz); ^{13}C NMR (CDCl_3 , 100 MHz) 13.43 (1J = 72.8 Hz, 5J = 15.7 Hz), 125.96, 125.99, 128.42, 129.49, 130.86, 131.72, 132.67, 133.50, 133.60, 134.49 (1J = 12.4 Hz), 135.26, 135.59, 135.83; ^{77}Se NMR (CDCl_3 , 76 MHz) 431.6, 234.7 ($^4J^{8}\text{Se}, ^1\text{Se}$) = 316.7 Hz). Anal. Calcd for $\text{C}_{17}\text{H}_{13}\text{Se}_2\text{Cl}$: C, 49.72; H, 3.19. Found: C, 49.77; H, 3.23.

1-(Methylselanyl)-8-(*p*-bromophenylselanyl)naphthalene (2e). Following a method similar to that for **2b**, **2e** gave 88% yield as a white solid: mp 90.0–91.0 °C; ^1H NMR (CDCl_3 , 400 MHz) 2.34 (s, 3H, $J(\text{Se}, \text{H})$ = 13.9 Hz), 7.23 (dd, 2H, J = 8.6, 2.2 Hz), 7.25 (t, 1H, J = 7.8 Hz), 7.34 (dd, 2H, J = 8.6, 2.2 Hz), 7.37 (t, 1H, J = 7.7 Hz), 7.62 (dd, 1H, J = 7.4, 1.2 Hz), 7.72 (dd, 1H, J = 7.5, 1.2 Hz), 7.74 (dd, 1H, J = 7.6, 1.2 Hz), 7.74 (dd, 1H, J = 7.6, 1.3 Hz); ^{13}C NMR (CDCl_3 , 100 MHz) 13.40 (1J = 72.7 Hz, 5J = 15.7 Hz), 121.57, 125.98, 126.01, 128.40, 129.57, 130.63, 131.77, 132.40 (1J = 10.7 Hz), 132.58, 134.38, 134.50 (1J = 11.6 Hz), 135.29, 135.79, 135.84; ^{77}Se NMR (CDCl_3 , 76 MHz) 432.4, 235.2 ($^4J^{8}\text{Se}, ^1\text{Se}$) = 313.9 Hz). Anal. Calcd for $\text{C}_{17}\text{H}_{13}\text{Se}_2\text{Br}$: C, 44.87; H, 2.88. Found: C, 44.89; H, 2.90.

1-(Methylselanyl)-8-[*p*-(ethoxycarbonyl)phenylselanyl]naphthalene (2f). Following a method similar to that for **2b**, **2f** gave 84% yield as a white solid: mp 83.5–84.0 °C; ^1H NMR (CDCl_3 , 400 MHz) 1.33 (t, 3H, J = 7.1 Hz), 2.30 (s, 3H, $J(\text{Se}, \text{H})$ = 14.6 Hz), 4.31 (q, 2H, J = 7.1 Hz), 7.27 (dd, 2H, J = 8.6, 2.2 Hz), 7.29 (t, 1H, J = 7.7 Hz), 7.37 (t, 1H, J = 7.7 Hz), 7.62 (dd, 2H, J = 7.4, 1.2 Hz), 7.72 (dd, 1H, J = 8.0, 1.0 Hz), 7.76 (dd, 1H, J = 7.3, 1.2 Hz), 7.81 (dd, 1H, J = 8.0, 1.4 Hz), 7.82 (dd, 1H, J = 8.3, 2.2 Hz); ^{13}C NMR (CDCl_3 , 100 MHz) 12.85 (1J = 74.5 Hz, 5J = 15.7 Hz), 14.29, 60.89, 126.03, 126.13, 127.99, 128.63, 130.14, 130.47, 130.80 (1J = 12.5 Hz), 131.34, 132.37, 135.52, 135.91, 137.77, 142.80, 166.31; ^{77}Se NMR (CDCl_3 , 76 MHz) 442.4, 239.2 ($^4J^{8}\text{Se}, ^1\text{Se}$) = 294.7 Hz). Anal. Calcd for $\text{C}_{20}\text{H}_{18}\text{Se}_2\text{O}_2$: C, 53.59; H, 4.05. Found: C, 53.61; H, 4.09.

1-(Methylselanyl)-8-(*p*-nitrophenylselanyl)naphthalene (2g). Following a method similar to that for **2b**, **2g** gave 81% yield as a white solid: mp 140.0–141.0 °C; ^1H NMR (CDCl_3 , 400 MHz) 2.29 (s, 3H, $J(\text{Se}, \text{H})$ = 13.9 Hz), 7.23 (dd, 2H, J = 9.0, 2.4 Hz), 7.37 (t, 1H, J = 7.7 Hz), 7.40 (t, 1H, J = 7.7 Hz), 7.63 (dd, 1H, J = 7.4, 1.0 Hz), 7.74 (dd, 1H, J = 8.2, 1.0 Hz), 7.86 (dd, 1H, J = 7.3, 1.4 Hz), 7.90 (dd, 1H, J = 8.1, 1.2 Hz), 7.97 (dd, 2H, J = 9.0, 2.4 Hz); ^{13}C NMR (CDCl_3 , 100 MHz) 12.47 (1J = 76.1 Hz, 5J = 14.8 Hz), 123.92, 126.11, 126.37, 126.65, 127.81, 130.02 (1J = 13.2 Hz), 130.67, 131.47, 132.42, 135.40, 136.00, 139.04 (1J = 9.9 Hz), 146.11, 146.74; ^{77}Se NMR (CDCl_3 , 76 MHz) 453.9, 240.1 ($^4J^{8}\text{Se}, ^1\text{Se}$) = 272.5 Hz). Anal. Calcd for $\text{C}_{17}\text{H}_{13}\text{Se}_2\text{N}_2\text{O}_2$: C, 48.48; H, 3.11; N, 3.33. Found: C, 48.66; H, 3.10; N, 3.27.

MO Calculations. Ab initio molecular orbital calculations were performed on an Origin computer using the Gaussian 94 program with 6-311+G(2d,p) and 3-21G* basis sets at B3LYP and/or HF levels.²² The σ values for H, C, and Se nuclei were calculated using the NMR key word of the program, and the natural charges (Qn) were calculated by the natural population analysis.²⁴

Acknowledgment. This work was supported by a Grant-in-Aid for Scientific Research (C) (No. 09640635) (W.N.) and on Priority Areas (A) (Nos. 09640635, 11120232, and 11166246) (W.N.) from the Ministry of Education, Science, Sports and Culture, Japan.

Supporting Information Available: Substituent effect on $\delta(\text{C})$ and $\delta(\text{Se})$ of the *p*- $\text{YC}_6\text{H}_4\text{Se}$ groups in **3–6** based on ab initio MO calculations. This material is available free of charge via the Internet at <http://pubs.acs.org>.

JO9903860